

2009

Application of vibration measurements and finite element model updating for structural health monitoring of ballasted railtrack sleepers with voids and pockets

Sakdirat Kaewunruen
RailCorp, sakdirat@hotmail.com

Alexander Remennikov
University of Wollongong, alexrem@uow.edu.au

Follow this and additional works at: <https://ro.uow.edu.au/engpapers>



Part of the [Engineering Commons](#)

<https://ro.uow.edu.au/engpapers/502>

Recommended Citation

Kaewunruen, Sakdirat and Remennikov, Alexander: Application of vibration measurements and finite element model updating for structural health monitoring of ballasted railtrack sleepers with voids and pockets 2009.

<https://ro.uow.edu.au/engpapers/502>

Chapter 12

**APPLICATION OF VIBRATION MEASUREMENTS AND
FINITE ELEMENT MODEL UPDATING FOR
STRUCTURAL HEALTH MONITORING OF BALLASTED
RAILTRACK SLEEPERS WITH VOIDS AND POCKETS**

Sakdirat Kaewunruen^{,1,2} and Alex M Remennikov¹*

¹School of Civil, Mining, and Environmental Engineering, Faculty of Engineering,
The University of Wollongong, Wollongong 2522 NSW, Australia

²RailCorp – Track Engineering, Level 13, 477 Pitt St, Sydney 2000 NSW, Australia

Abstract

Although vibration measurements are very useful and common in practice nowadays in many applications related to mechanical, civil, and aerospace engineering, the utilisation in railtrack infrastructure and facilities is not widely established. This chapter deals with the application of vibration measurements and finite element model updating to the assessment of ballasted railtrack sleepers, in particular with a void and pocket condition. It describes the concept of vibration measurements and the understanding into the dynamic behaviour of ballasted railtrack sleepers. It discusses briefly on the development of finite element model of in-situ sleeper and its updating. Then, the application to structural health monitoring of the rail-track sleepers is demonstrated. Dynamic load effects on the in-situ concrete sleepers in a railway track system are very significant and highly regarded in the viewpoint of structural engineers since the resonant excitation frequencies amplify the vibration magnitudes and cause cracking of railway concrete sleepers. New concept for the design criteria of railway concrete sleepers considers such resonant effects. As one of the main components of railway tracks, ballast interacts with the sleepers and influences the dynamic characteristics of railway sleepers, as well as the dynamic modulus of railtracks. The ballast support configurations are often changed by the effects of wheel load, breakage of gravel, or loss of confinement, which therefore creates voids and pockets underneath railway sleeper. This chapter presents a comparison between the experimental investigation on free vibration behaviour of an in-situ railway concrete sleeper with voids and pockets underneath, and the numerical prediction

* Corresponding Author: Sakdirat Kaewunruen; School of Civil, Mining, and Environmental Engineering, Faculty of Engineering, University of Wollongong, Wollongong, 2522 NSW, Australia; Tel: 02 8922 1151 Fax: 02 8922 1154; E-mail: sakdirat@hotmail.com; sak.kaewunruen@railcorp.nsw.gov.au

incorporating sleeper/ballast interaction. It is aimed at demonstrating the development and application of the vibration measurement and model updating to railway engineering practice. Using finite elements, Timoshenko-beam and spring elements were used in the in-situ railway concrete sleeper modelling, whereas the voids and pockets could be superiorly treated. This model had been proven its effectiveness for predicting the free vibration characteristics of in-situ sleepers under different circumstances. In addition, the modal testing results have clearly exhibited that the simplified approach is ample to predict the natural vibrations of voided railway concrete sleepers. This study has led to the prediction and understanding of dynamic characteristics of railway concrete sleepers under various configurations of voids and pockets.

Key words: Free vibrations; In situ concrete sleepers; Rail pad; Ballast; Voids and pocket; Modal testing; Vibration measurement; Finite element model updating.

1. Introduction

Railway tracks consist of several components grouped into two categories: substructure and superstructure. The substructure includes ballast, sub-ballast, and subgrade, while the superstructure includes sleepers (or sometimes called 'tie'), rail pads, fasteners, and rails. Figure 1 schematically depicts the typical ballasted railway tracks. Rolling stocks usually ride over the rails to transport passengers, goods, etc. The burden of vehicle and transported mass will transfer to axle, to wheel, and then to track structures. The loading conditions acting on railway tracks are normally time dependent since the wheels interact with rails, causing dynamic effects. The dynamic loads often excite the railway track components with increased magnitudes at specific frequencies associated with such components. It is found that the railway concrete sleepers deteriorate greatly when they are subjected to dynamic loads at their resonant frequencies, especially in flexural modes of vibration (Barke and Chiu, 2005; Remennikov and Kaewunruen, 2007). Therefore, resonant characteristics of in-situ railway concrete sleepers are essential in their own analysis and design.

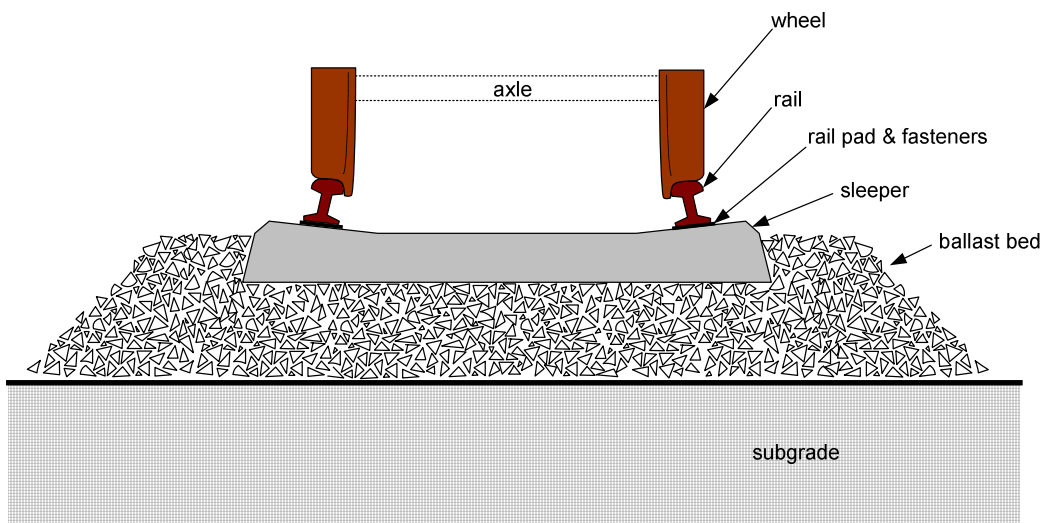


Figure 1. Typical railway tracks

Based on a number of research studies, it has been found that the resonant vibrations of sleepers affect not only the sleepers themselves, but also the wheel–rail interaction forces (Clark et al., 1982; Knothe and Grassie, 1993; Remennikov and Kaewunruen, 2007). Grassie and Cox (1984) presented the dynamic responses to high frequency excitation of a railway track. They found that the higher pad stiffness tends to increase the contact forces, and that the typical corrugation-passing frequencies (e.g. 750 Hz for a corrugation of 60 mm wavelength and train speed of 45 m/s) are most likely to cause much damage on concrete sleepers at their second and third dynamic mode shapes. It should be noted that the normal train operation causes the dynamic forces at the frequency bandwidth between 0 and 20 Hz for sprung mass and between 20 and 125 Hz for unsprung mass. In particular, some defects on wheels or rails, such as corrugations, bad welds, or wheel flats, can create the forces with a variety of frequency spans varying from 0 to 2,000 Hz, depending on the train speeds and type of defects (Esveld, 2001; Remennikov and Kaewunruen, 2007). These dynamic force frequencies are often matched with the resonances of railway concrete sleepers, resulting in the accelerated deterioration of such elements as previously described. Therefore, it is imperative to investigate and monitor the dynamic characteristic of railway concrete sleepers under different circumstances. Structural health monitoring can be found by two main investigations: experimental and analytical studies. The most common practice involves the experimental modal analysis whereas the vibration measurement is performed to obtain modal parameters. The analytical investigations are often achieved by finite element approach. However, the integration between experimental and analytical studies can lead to calibrated models, which can be used for structural condition assessment and monitoring. This procedure is so-called ‘finite element model updating’ as described in Figure 2 (Friswell and Mottershead, 1995).

Esveld (2001) discovered that the ballast breakage increases substantially at a track resonance, so-called in-phase vibration. This phenomenon causes the voids and pockets, or even the poor packing of ballast support underneath railway concrete sleepers (Barke and Chiu, 2005; Kaewunruen and Remennikov, 2007a). A sleeper having voids and pockets underneath is hereafter referred to as ‘voided sleeper’. There are several investigations on free vibrations of in-situ railway sleeper in track system. Dahlberg and Nielsen (1991) and Nielsen (1991) developed an analytical model for analysing the dynamic behaviors of concrete sleepers in both free-free and in-situ conditions, using the Wittrick-Williams bisection method. This method makes it inconvenient to handle with the variations of voids and pockets. Grassie (1995) carried out experiments and a two-dimensional dynamic modelling for vibration analysis of concrete sleepers in free-free condition. Based on these studies, the Timoshenko beam element was the best approximation for the concrete sleepers, even though the elastic properties of prestressed concrete sleepers may not be exact. Noteworthy, the sleepers are generally designed using ‘*permissible stress*’ concept whereas their behaviour under service loads is elastic (Kaewunruen and Remennikov, 2008). Therefore, the model is accurate to sufficiently explain the sleeper dynamic behaviour. The effects of rail pad parameters on the dynamic behaviours of in-situ railway concrete sleepers are significant, and have been previously presented (Kaewunruen and Remennikov, 2006a). Recently, Plenge and Lammering (2003) have investigated the influence of a voided sleeper on the frequency response functions of the sleeper, two adjacent sleepers, and a track segment. The test programs dealt only with sleepers B70W60, designed in accordance with the German standard. It was found that the partially supported sleeper dramatically increases

the receptance level (at sleeper end) at frequencies varying from 0 to 150 Hz whilst at frequencies beyond 150 Hz the receptance level decreases slightly. Moreover, the voids and pockets would also allow the sleepers to vibrate freely with greater magnitudes and lead to larger crack widths or fatigue (Kaewunruen and Remennikov, 2007a). Based on the literature survey, the influence of voids and pockets on the dynamic behaviors of local railway concrete sleepers has yet been investigated, although it is vital to the damage detection and structural health monitoring of the in-situ railway concrete sleepers in particular. In addition, although the sleepers are pressed down onto the ballast when a train passes, no one can guarantee whether under any circumstances the voids (at least most of them) are closed and the ballast fully supports the sleepers at the train passages. The fundamental reason of derailment and track overturning can be of numerous theories. One possible way is the high risk of overturning instability of railway tracks whereas the resonances due to void effects could enhance the overturning instability of global tracks.

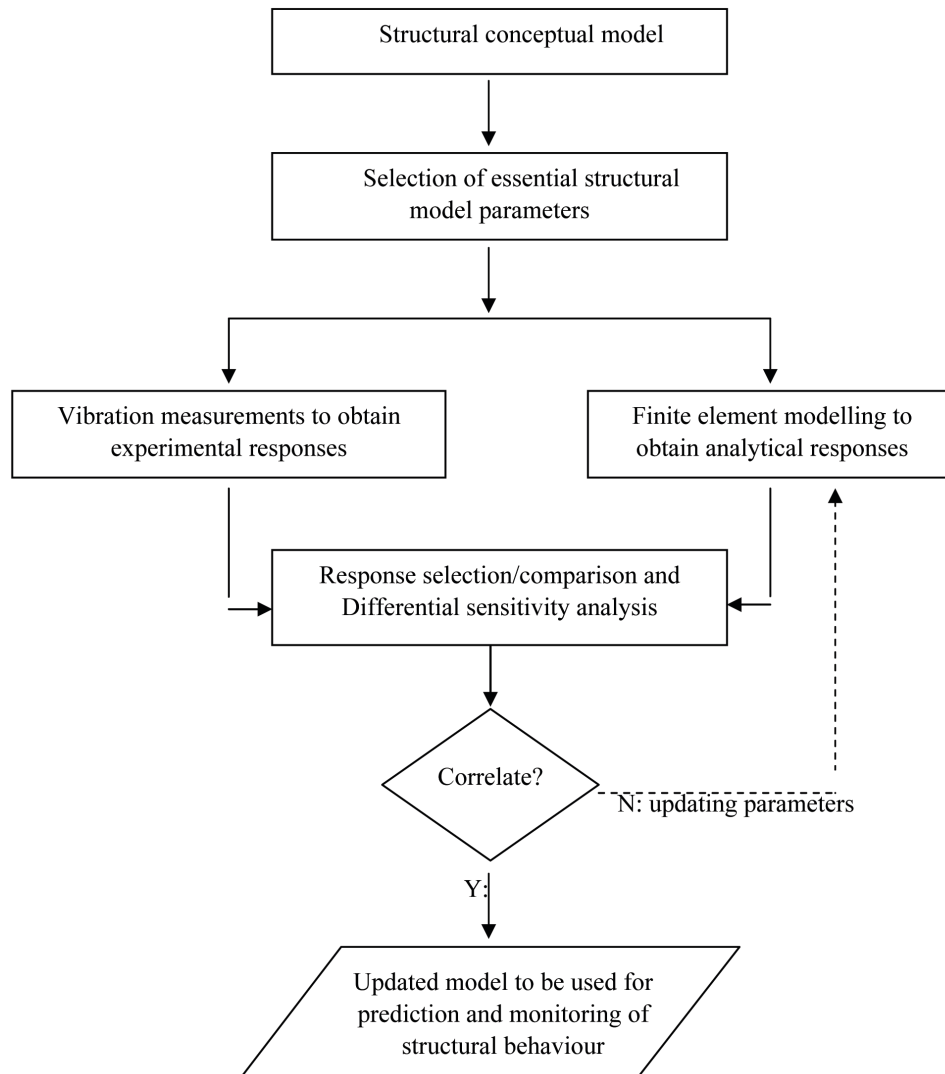


Figure 2. Flowchart of finite element model updating procedure

This chapter presents the experimental and numerical studies for the better understanding into free vibration characteristics of voided railway concrete sleepers. A type of void configurations was selected for demonstration in this study, which is called ‘the single-side hover voided sleeper’ as illustrated in Figure 3. Modal testing was employed for the dynamical experiments on a selected Australian-manufactured concrete sleeper. The concrete sleeper modeled herein is the modified Australian standard gauge sleeper type, adopted from previous work (Kaewunruen and Remennikov, 2006a; 2007a). This type of sleepers is the in-situ mono-block cross tie usually used in Australian ballasted railway tracks. The main aim of this study was to calibrate the prediction model for the dynamic behaviors of in-situ sleepers in which the in-situ conditions and the sleeper/ballast interaction had been also taken into account. The voided sleepers were considered as beams on elastic foundation of the Winker type. The model was developed using the finite element package, STRAND7. Two-dimensional beam element, considering shearing effects, was used to model the concrete sleeper taking into account the shear deformation and rotational inertia. The ballast-support system and rail pad were modeled using elastic support feature and spring elements, respectively. The elastic support feature allows some changes in order to investigate the effects of the potential voids. The numerical results have been compared against the dynamically experimental results. In practice the sleeper is also connected to the rails and that influences the dynamic behaviours. Since the case study has been simplified, the normalized trends of natural frequencies of the sleeper are displayed to give a better insight into the dynamic stability and behaviors of the voided railway concrete sleeper in the actual tracks. Vibration measurements and finite element model updating provide a successful tool for monitoring the dynamic behaviour of railway sleepers with voids and pockets underneath them. These investigations have resulted in the further studies on dynamic characteristics of other configurations of voided railway concrete sleepers (Kaewunruen and Remennikov, 2007c).

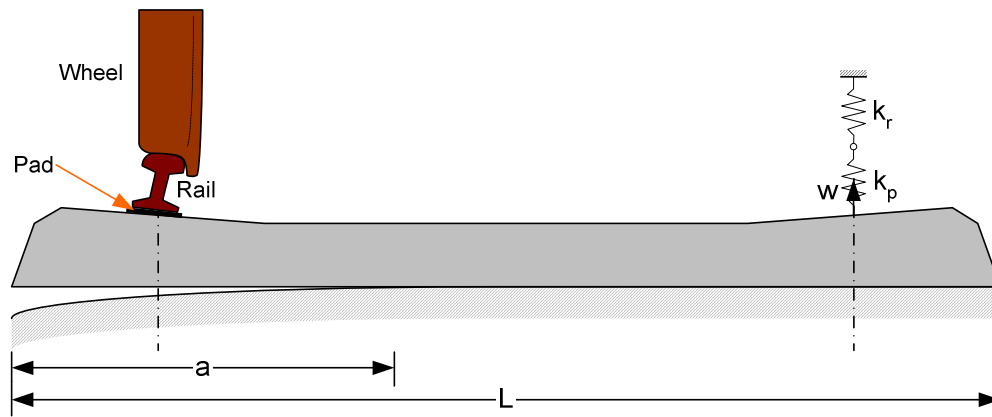


Figure 3. Schematic model of a type of voided railway concrete sleepers (single-side hover)

2. Contemporary Design Concept of Railway Sleepers

At present, many organisations (e.g. American Railway Engineering and Maintenance-of-Way Association, Standards Australia, European Committee for Standardization, and International Union of Railways) address the design methodology of railway sleepers. Most of them prescribe a design methodology for concrete sleepers using permissible stress design concept. The *life cycle* of the sleepers based on this standard is 50 years. The design process relies on the permissible or allowable stress of materials. A load factor is used to increase the static axle load to incorporate dynamic effects. The design load is termed '*combined quasi-static and dynamic load*' which has a specified lower limit of 2.5 times static wheel load. Load distribution to a single sleeper, rail seat load, and moments at rail seat and centre can be obtained using tables provided in AS1085.14. It should be noted that the ballast pressure underneath sleepers is not permitted to exceed 750 kPa for high-quality ballast. Factors to be used for strength reduction of concrete and steel tendons at transfer and after losses can be found in the standard, ranging between 40% to 60% reduction. However, the minimum pre-camber compressive stress at any cross-section through the rail seat area is set at 1 MPa after all losses (loaded only from prestress). It should be noted that 25% loss of prestress is to be assumed for preliminary design or when there is no test data. A lower level of 22% loss has been generally found in final design of certain types of sleepers (Standards Australia, 2003).

Past practice has indicated that utilisation of this permissible stress design concept is adequate for flexural strength design. AS1085.14 (Standards Australia, 2003) states that if the design complies with AS1085.14, there is no need for consideration to checking stresses other than flexural stresses, because the permissible stress design concept limits the strengths of materials to comparatively low values compared to their true capacity. Under the design loads, the material is kept in the elastic zone so there is no permanent set. In particular, sleepers that comply with AS1085.14 have all cross sections of the sleepers fully in compression, under either pre-camber or design service loads. This approach ensures that an *infinite* fatigue life is obtained and *no* cracking occurs.

As a result, the railway sleepers designed compliant with the permissible design concept are behaving only in elastic zone. The use of Timoshenko beam theory has then become the most suitable means for simplified dynamic analysis of railway sleepers. In fact, experimental test results have shown that the sleepers designed based on this concept have a significant reserve of strength within their 50 year life cycle under normal service loads (Remennikov et al., 2007). This permissible design concept is considered to be based on empirical methods that rely on simplistic impact factors to roughly represent dynamic forces by trains. The impact factor is obtained from short-term on-track measurement, which is very limited for long-term risk assessment of rail tracks. These have led to the development of a new limit states design concept for railway sleepers. This topic currently attracts a number of research funds and is being investigated under a research framework of Australia Centre for Railway Engineering and Technologies (Rail-CRC) or currently called 'CRC for Rail Innovation'.

3. Vibration Measurements

Experimental modal analysis (EMA) or modal testing is a non-destructive testing strategy based on vibration responses of the structures. Over the past decade, the modal testing has

become an effective means for identifying, understanding, and simulating dynamic behaviour and responses of structures. One of the techniques widely used in modal analysis is based on an instrumented hammer impact excitation. By using signal analysis, the vibration response of the structures to the impact excitation is measured and transformed into frequency response functions (FRFs) using Fast Fourier Transformation (FFT) technique. Subsequently, the series of FRFs are used to extract such modal parameters as natural frequency, damping, and corresponding mode shape. In a wide range of practical applications the modal parameters are required to avoid a resonance in structures affected by external periodic dynamic loads. Practical applications of modal analysis span over various fields of science, engineering and technology. In particular, numerous investigations related to aeronautical engineering, automotive engineering, and mechanical engineering have been reported (Kaewunruen and Remennikov, 2005; Remennikov and Kaewunruen, 2005). In this study, the modal testing is sound and has been employed in the experiments.

The test specimen was the prestressed concrete sleeper designed in accordance with AS1085.14-2003 (Standards Australia, 2003). The dimensions and masses of the test sleeper are tabulated in Table 1. The sleeper is the heavy-duty sleeper type provided by ROCLA. The excitation points were located on the top surface of the sleeper at every 150 mm along the perimeter. It is important to note that the number of these positions should be sufficient to represent the vibration modes of interest. In this case, an accelerometer had a fixed position whilst an instrumented impact hammer was roved along the excitation points. Figure 4 shows the experimental setup of the voided sleeper.



Figure 4. Experimental setup of a voided railway concrete sleeper

Table 1. Dimensions and masses of the test sleeper*

Sleeper Type	Mass (kg)	Total length (m)	At railseat (m)		At centre (m)	
			width	depth	width	depth
standard	206.0	2.50	0.20	0.23	0.21	0.18

*adopted from [16]

From previous experiments (Remennikov and Kaewunruen, 2006), the best position for installing the accelerometer is at the end of the sleeper. At this point, the FRFs recorded are clear at all modes of vibration without any noise. The instruments used in these experiments include a PCB accelerometer, the PCB impact hammer, and the Bruel&Kjaer PULSE vibration analyser. The accelerometer was mounted at both sleeper ends for two series of dynamic testings, in order to investigate the discrepancy when using the FRFs obtained from different ends. Using the instrumented hammer to excite vibrations in the sleeper over the frequency range 0 to 1600 Hz, the 10-time average vibration responses represented by the FRFs were obtained using the PULSE system. Then, processing the recorded FRFs by STARModal gave the natural frequencies and modal damping constants of the sleeper. All procedures were performed twice per a voided sleeper as the percentage of sleeper/ballast contact zone (artificial void) would vary from full contact ($a/L = 0.00$), 90% ($a/L = 0.10$), 80% ($a/L = 0.20$), 70% ($a/L = 0.30$), and 60% ($a/L = 0.40$), see Figure 4. It was also found that the instability of the voided sleeper occurs at about 58% sleeper/ballast contact where the overhanging part of the sleeper tends to tip over. This was the reason why the experimental data were limited up to $a/L = 0.40$. The experimental techniques in details can be found in Remennikov and Kaewunruen (2006).

4. Finite Element Modelling and Updating

A dynamic finite element simulation of the in-situ railway concrete sleeper, which was developed earlier in two dimensions and successfully validated (Kaewunruen and Remennikov, 2006a; 2007a), has been adopted for this study. The railway concrete sleeper is modelled using fifty Timoshenko beam elements with a trapezoidal cross-section while rail pads and ballast systems were modelled as a spring-dashpot element and the elastic beam support features in STRAND7 (G+D Computing, 2002; 2005). The elastic support feature allows the changes in any element along the beam, making it possible to investigate any type of potential void configurations. The standard input data and engineering properties of those components have been adopted from previous investigations as tabulated in Table 2 (Dahlberg and Nielsen, 1991; Cai, 1992; Grassie, 1995; Sadeghi, 1997; Kumaran et al., 2003; Kaewunruen and Remennikov, 2006a; 2007a; Remennikov and Kaewunruen, 2006). The in-situ boundary condition is simplified using spring elements as rail pads connected to rails. Verifications of the model have been done earlier in both free-free and in-situ conditions. The results of either eigenvalues or eigenmodes are in very good agreement with the previous findings in (Kaewunruen and Remennikov, 2006a). The results have clearly proven that the finite element model and the simplified approach are capable of predicting the dynamic characteristics of in-situ railway concrete sleepers in a track system.

Table 2. Properties used in concrete sleeper validation model*

Parameter lists		
Flexural rigidity	$EI_c = 4.60, EI_r = 6.41$	MN/m ²
Shear rigidity	$\kappa GA_c = 502, \kappa GA_r = 628$	MN
Ballast stiffness	$k_b = 13$	MN/m ²
Effective stiffness	$k_e = 17$	MN/m
Sleeper density	$\rho_s = 2,750$	kg/m ³

*adopted from [11]

The voids and pockets of ballast underneath railway concrete sleeper are varying depending on many factors such as railway tracks, dynamic loads, and substructure strength. This chapter highlights only a type of voided sleepers when a side of the sleeper is hovering, and whereas the experimental results are available. The present model is developed based on experimental and numerical validations of an Australian standard gauge sleeper, which is identical to the test specimen. The numerical analysis has been carried out, by omitting the elastic support stiffness step by step. The numerical results based on the standard data input are given in Table 3. However, in the experiments, the concrete sleeper was simply laid on the ballast and a sample of such sleeper batch was performed under the static ultimate load (Kaewunruen and Remennikov, 2006b; 2006c). These static ultimate tests also result in the model updating by correcting the effective elastic modulus of concrete sleeper ($EI = 8.4$) and setting the rail pad spring to nil ($k_e = 0$). The numerical results of the updated finite element model based on Grassie's results (1995) are given in Table 4. The updated model excludes the rail assembly to imitate the actual experimental setup. It should be noted that the experimental modal testing was first performed to identify structural parameters of the sleeper. Then, the finite element model was developed using available data from the manufacturer. The model was then updated through the comparison of modal parameters and dynamic responses as shown in Figure 2 (Friswell and Mottershead, 1995).

Table 3. Natural frequencies of standard sleepers under various percent sleeper/ballast contacts

% sleeper/ballast contact	Frequencies (Hz)						
	Rigid Body Motion		Flexural Vibrations				
	Translation	Rotation	Mode 1	Mode 2	Mode 3	Mode 4	Mode 5
full contact	68.66	70.59	122.21	313.44	607.3	997.47	1485.49
90 ($a/L=0.1$)	69.28	63.82	119.91	312.86	607.08	997.36	1485.42
80 ($a/L=0.2$)	69.27	59.09	119.53	312.79	606.93	997.21	1485.32
70 ($a/L=0.3$)	69.17	55.72	119.44	312.30	606.65	997.15	1485.27
60 ($a/L=0.4$)	68.83	53.43	118.75	311.72	606.61	997.00	1485.17
50 ($a/L=0.5$)	51.85	68.06	117.50	311.60	606.35	996.89	1485.10
40 ($a/L=0.6$)	50.76	66.69	116.36	311.46	606.08	996.79	1485.03
30 ($a/L=0.7$)	50.04	64.61	115.90	310.87	606.04	996.63	1484.93
20 ($a/L=0.8$)	49.60	61.68	115.85	310.38	605.76	996.57	1484.88
10 ($a/L=0.9$)	49.34	57.66	115.11	310.32	605.62	996.42	1484.78
free-free	-	-	111.60	307.38	602.12	994.46	1484.33

Table 4. Natural frequencies of the updated sleeper model under various percent sleeper/ballast contacts

% sleeper/ballast contact	Frequencies (Hz)						
	Rigid Body Motion		Flexural Vibrations				
	Translation	Rotation	Mode 1	Mode 2	Mode 3	Mode 4	Mode 5
full contact	48.29	48.27	145.83	382.13	744.09	1227.32	1831.12
90 ($a/L=0.1$)	48.28	38.96	143.97	381.62	743.90	1227.23	1831.06
80 ($a/L=0.2$)	48.23	30.56	143.65	381.57	743.79	1227.11	1830.98
70 ($a/L=0.3$)	48.03	23.19	143.57	381.18	743.56	1227.06	1830.94
60 ($a/L=0.4$)	47.54	17.12	142.96	380.71	743.53	1226.94	1830.86
50 ($a/L=0.5$)	46.53	12.14	141.83	380.61	743.31	1226.85	1830.80
40 ($a/L=0.6$)	44.65	08.08	140.75	380.50	743.10	1226.76	1830.74
30 ($a/L=0.7$)	41.43	04.87	140.24	380.03	743.06	1226.64	1830.66
20 ($a/L=0.8$)	36.18	02.43	140.19	379.64	742.84	1226.59	1830.62
10 ($a/L=0.9$)	27.61	00.80	139.71	379.59	742.72	1226.47	1830.54
free-free	-	-	137.63	379.07	742.53	1226.38	1830.48

5. Results and Discussions

The simplified test bed has been used to clearly identify the effect of voids and pockets on the dynamic behaviours of railway sleepers. The results of vibration tests for the test sleeper are depicted in Tables 5-6. In these tables, the first four bending modes of vibration are presented. The results in Table 5 were obtained from the first vibration test when the accelerometer was

mounted on the hovering end, whilst Table 6 shows the modal results of the test when the accelerometer was placed on the other end. It is very clear that both results are fairly close at all cases, proving the precision of vibration testing methodology. It is also found from Tables 4-6 that the updated model can accurately predict the dynamic characteristics of the voided sleepers. The discrepancies found are less than 5% for the flexural cases and about 10% for the rigid body motions. However, the experimental results are limited to only flexural vibrations up to 1,600 Hz, or on the other hand they accommodate only the first four modes associated with impact loads on railway tracks (Kaewunruen and Remennikov, 2007b). Comparing experimental results between free-free condition and the case with ballast support in Tables 5 and 6, it is found that the ballast support played a major role in escalating the damping values of all vibration modes. The increment of damping constant due to sleeper-ballast interaction could be up to 40 times. The damping topic is however not in the scope of this chapter and will not be described at this state. By the way, it should be noted that the mode shapes of ballasted sleepers tabulated in Tables 5 and 6 were quite difficult to identify since some mode shapes were sometimes too closely spaced between each other complex mode of vibration (e.g. torsion). In this study, the experiments on the ballast test bed were stopped at 60 percent of sleeper/ballast contact where beyond this point the static instability can be observed. Due to the overhang mass, the dynamic hardening phenomenon of rigid body dynamics may occur. Based on the FRFs obtained from the experiments, the rigid-body modes of vibration can be identified. The translation mode can be extracted as tabulated in Table 7. Nonetheless, it is very hard to discover the rotation modes in the low frequency range because the FRFs were obtained in the large frequency band and the zoom function feature was not used during the measurements. It is found that the experimental results of the rotation mode are slightly different from the numerical ones. However, the normalized results, as shown in Figure 5, tend to be similar.

Table 5. Modal parameters of ROCLA Heavy Duty with different single hover conditions (001Z Response)

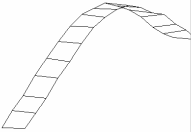
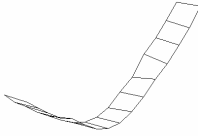

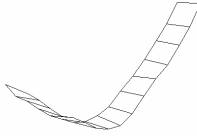
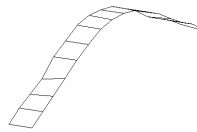
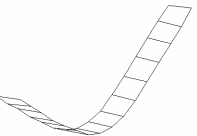
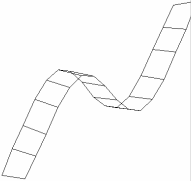
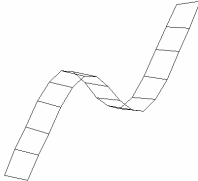
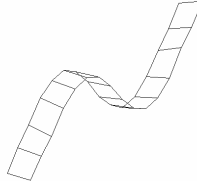
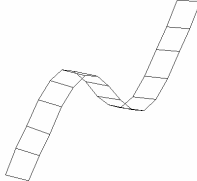
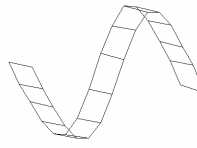
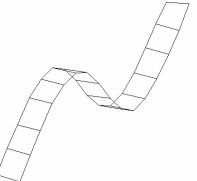

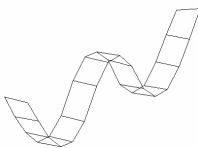
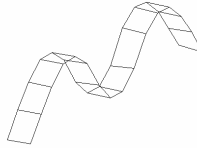
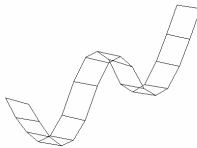
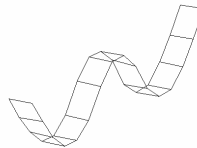
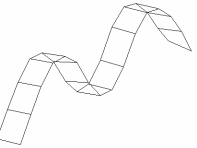
Mode	Full Contact		90% Contact ($a/L=0.1$)		80% Contact ($a/L=0.2$)		70% Contact ($a/L=0.3$)		60% Contact ($a/L=0.4$)		Free-Free	
	Frequency (Hz)	Damping (%)	Frequency (Hz)	Damping (%)	Frequency (Hz)	Damping (%)	Frequency (Hz)	Damping (%)	Frequency (Hz)	Damping (%)	Frequency (Hz)	Damping (%)
1												
	150.39	8.460	147.61	9.338	145.92	4.435	143.93	10.38	143.34	7.485	135.71	266.37m
2												
	414.93	2.586	414.64	2.531	414.57	2.472	414.49	2.546	409.37	1.517	404.83	298.96m
3												
	775.56	1.624	775.61	1.528	775.40	1.577	775.61	1.644	775.98	1.450	767.84	279.37m

Table 5. Continued.

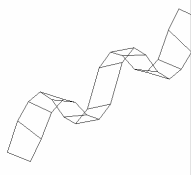
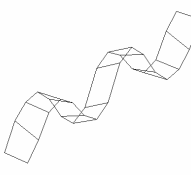
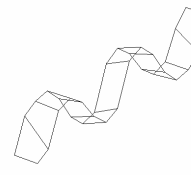
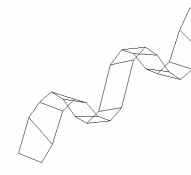
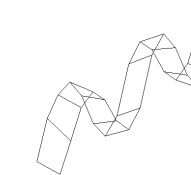
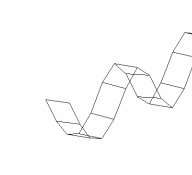
Mode	Full Contact		90% Contact ($a/L=0.1$)		80% Contact ($a/L=0.2$)		70% Contact ($a/L=0.3$)		60% Contact ($a/L=0.4$)		Free-Free	
	Frequency (Hz)	Damping (%)	Frequency (Hz)	Damping (%)	Frequency (Hz)	Damping (%)	Frequency (Hz)	Damping (%)	Frequency (Hz)	Damping (%)	Frequency (Hz)	Damping (%)
4												
	1,207.18	1.628	1,206.08	1.543	1,207.79	1.435	1,208.31	1.429	1,204.21	1.002	1,198.36	288.91m

Table 6. Modal parameters of ROCLA Heavy Duty with different single hover conditions (017Z Response)

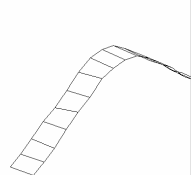
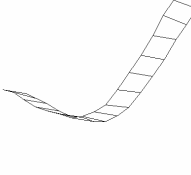
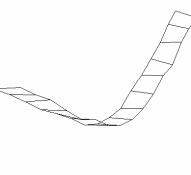
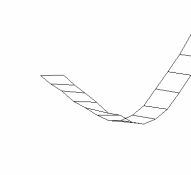
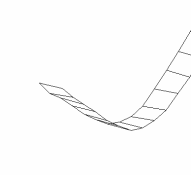
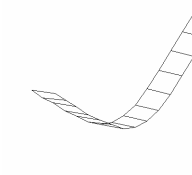
Mode	Full Contact		90% Contact ($a/L=0.1$)		80% Contact ($a/L=0.2$)		70% Contact ($a/L=0.3$)		60% Contact ($a/L=0.4$)		Free-Free	
	Frequency (Hz)	Damping (%)	Frequency (Hz)	Damping (%)	Frequency (Hz)	Damping (%)	Frequency (Hz)	Damping (%)	Frequency (Hz)	Damping (%)	Frequency (Hz)	Damping (%)
1												
	148.62	7.520	147.70	8.906	147.63	9.823	146.19	9.496	145.89	8.746	135.71	266.37m

Table 6. Continued.

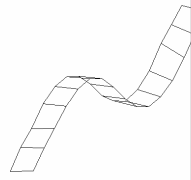
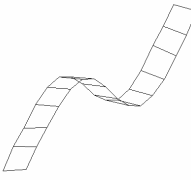
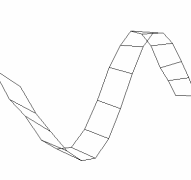
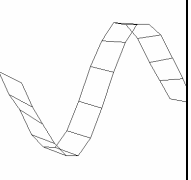
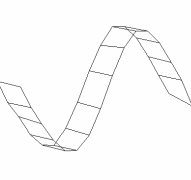
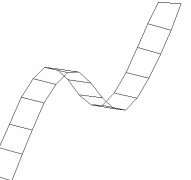
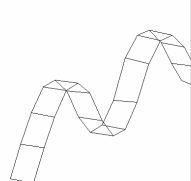
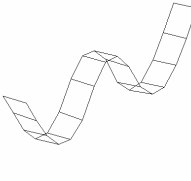
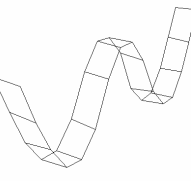
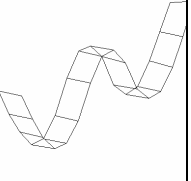
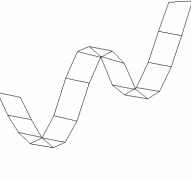
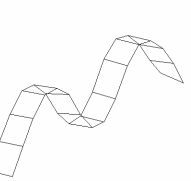
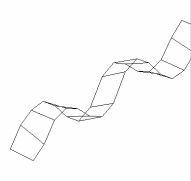
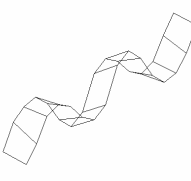
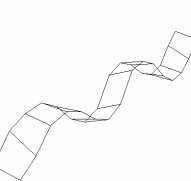
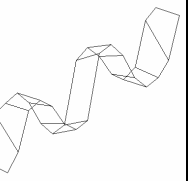
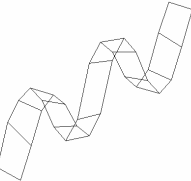
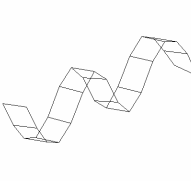
Mode	Full Contact		90% Contact ($a/L=0.1$)		80% Contact ($a/L=0.2$)		70% Contact ($a/L=0.3$)		60% Contact ($a/L=0.4$)		Free-Free	
	Frequency (Hz)	Damping (%)	Frequency (Hz)	Damping (%)	Frequency (Hz)	Damping (%)	Frequency (Hz)	Damping (%)	Frequency (Hz)	Damping (%)	Frequency (Hz)	Damping (%)
2												
	415.61	2.720	414.97	2.632	414.94	2.602	414.57	2.519	409.28	1.603	404.83	298.96m
3												
	775.77	1.602	775.53	1.627	775.21	1.575	775.28	1.622	775.69	1.426	767.84	279.37m
4												
	1,205.53	1.512	1,206.22	1.442	1,207.03	1.439	1,208.72	1.598	1,204.07	1.006	1,198.36	288.91m

Table 7a. Rigid body motion of ROCLA Heavy Duty with different single hover conditions (001Z Response)

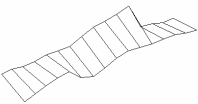
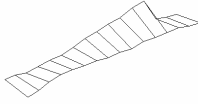
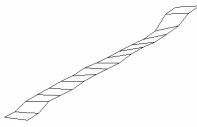
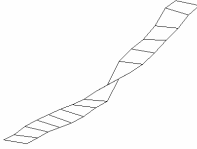
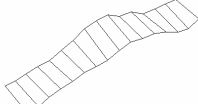
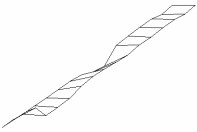
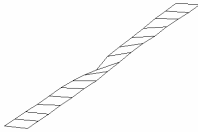
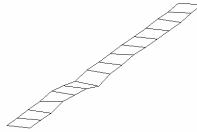
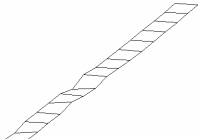
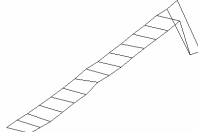
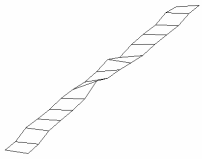
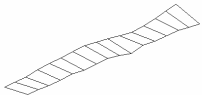
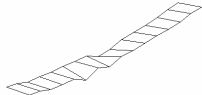
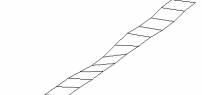
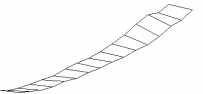
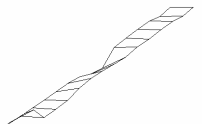
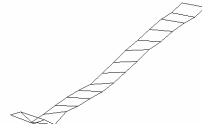
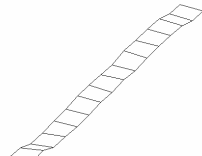
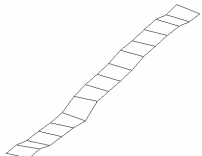
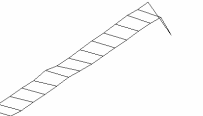
Mode	Full Contact		90% Contact ($a/L=0.1$)		80% Contact ($a/L=0.2$)		70% Contact ($a/L=0.3$)		60% Contact ($a/L=0.4$)	
	Frequency (Hz)	Damping (%)	Frequency (Hz)	Damping (%)	Frequency (Hz)	Damping (%)	Frequency (Hz)	Damping (%)	Frequency (Hz)	Damping (%)
T										
	41.75	4.23	41.69	4.99	37.72	6.97	37.55	7.36	32.05	1.58
R										
	41.70	7.44	39.36	3.94	29.83	2.74	29.66	4.28	20.47	4.06

Table 7b. Rigid body motion of ROCLA Heavy Duty with different single hover conditions (017Z Response)

Mode	Full Contact		90% Contact ($a/L=0.1$)		80% Contact ($a/L=0.2$)		70% Contact ($a/L=0.3$)		60% Contact ($a/L=0.4$)	
	Frequency (Hz)	Damping (%)	Frequency (Hz)	Damping (%)	Frequency (Hz)	Damping (%)	Frequency (Hz)	Damping (%)	Frequency (Hz)	Damping (%)
T										
	42.12	2.39	42.02	2.42	42.54	2.84	40.98	3.43	36.57	4.56
R										
	40.71	2.47	39.57	8.68	30.32	5.93	29.72	3.67	20.74	4.24

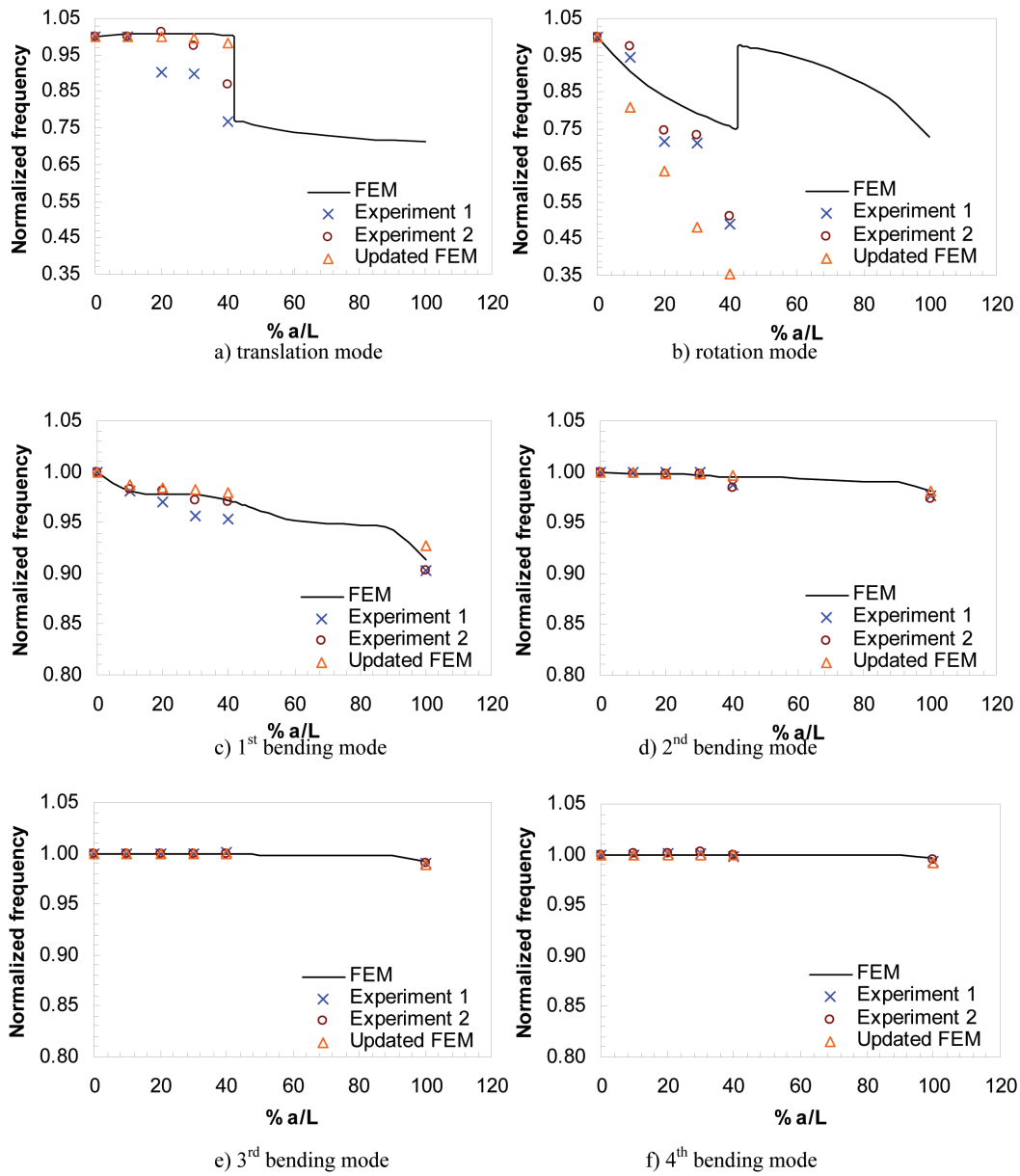


Figure 5. Normalized modal changes of a voided railway concrete sleeper

Figure 5 presents the comparison between experimental and numerical results of dynamic behaviours of the voided sleeper in terms of normalized frequencies. At all cases, the trend of dynamic characteristics of the voided sleeper using the simplified model is very similar to the experimental modal results. The discrepancy in the rigid body dynamics is attributable to the instability of the test sleeper corresponding to particular modal displacements. The experimental results clearly confirm the dynamic softening phenomenon in rigid body modes associated with those from the updated finite element model (beam on elastic foundation). The dynamic softening phenomenon occurs when the natural frequency diminishes as the amplitude of vibration or other parameters. It is found that out of all flexural modes, the most

significant change in natural frequencies among all void conditions was the first bending mode. The maximum frequency increase was about 10 percent found in the numerical results and about 11 percent noticed in the experimental results. However, it was found that at higher resonant frequencies, the effect of voids and pockets was remarkably decreased to only two percent difference in eigenfrequencies of the second to fourth vibration modes. Accordingly, the finite element model is sufficient for the dynamic analysis of voided railway concrete sleepers.

In addition, it is discovered from the numerical analyses considering the rail assembly (in-situ sleeper model) that there are cross-over phenomena of dynamic mode shapes of voided railway concrete sleeper in a track system due to static instability during the transition of sleeper/ballast contact from 60 to 50 percent (a/L 0.4 to 0.5). These phenomena involve only rigid body dynamics: translation and rotation, as depicted in Figure 6. For the translation mode, the displacements of the translation eigenvectors at both rail seats tend to exist in the same direction. In contrast, the directions of displacement vectors at rail seats behave conversely for the rotation mode. It is found in Figure 6 that when the void expands, the lowest mode will suddenly shift from rotation to translation. Simultaneously, the subsequent mode will change from translation back to rotation. The reason is that the translation mode relies mostly on the allowable displacements of springs (rail pads) at rail seats (Kaewunruen and Remennikov, 2007a). As shown in Table 3, when the void initiates, the over hanging mass pre-stresses on rail seat springs, resulting in the slightly higher translation frequencies since it becomes a stiffer system to translate. As the rotation is prone to the void size, the rotation frequencies reduce by degrees. When the void is larger enough to induce static instability of the continuum sleeper in the track system, it causes the cross over phenomena when over hanging mass is large enough to sway the sleeper to the void region and the sleeper forms a new stable configuration. The new stable configuration allows translation but rotation, so that the translation mode shifts down to the lowest resonance, and vice versa. This understanding is fundamentally important to the dynamic health monitoring of a railway track and its components. Also, this study has led to the numerical prediction associated with the influences of voids/pockets and contact mechanisms underneath the sleeper (Kaewunruen and Remennikov, 2007c).

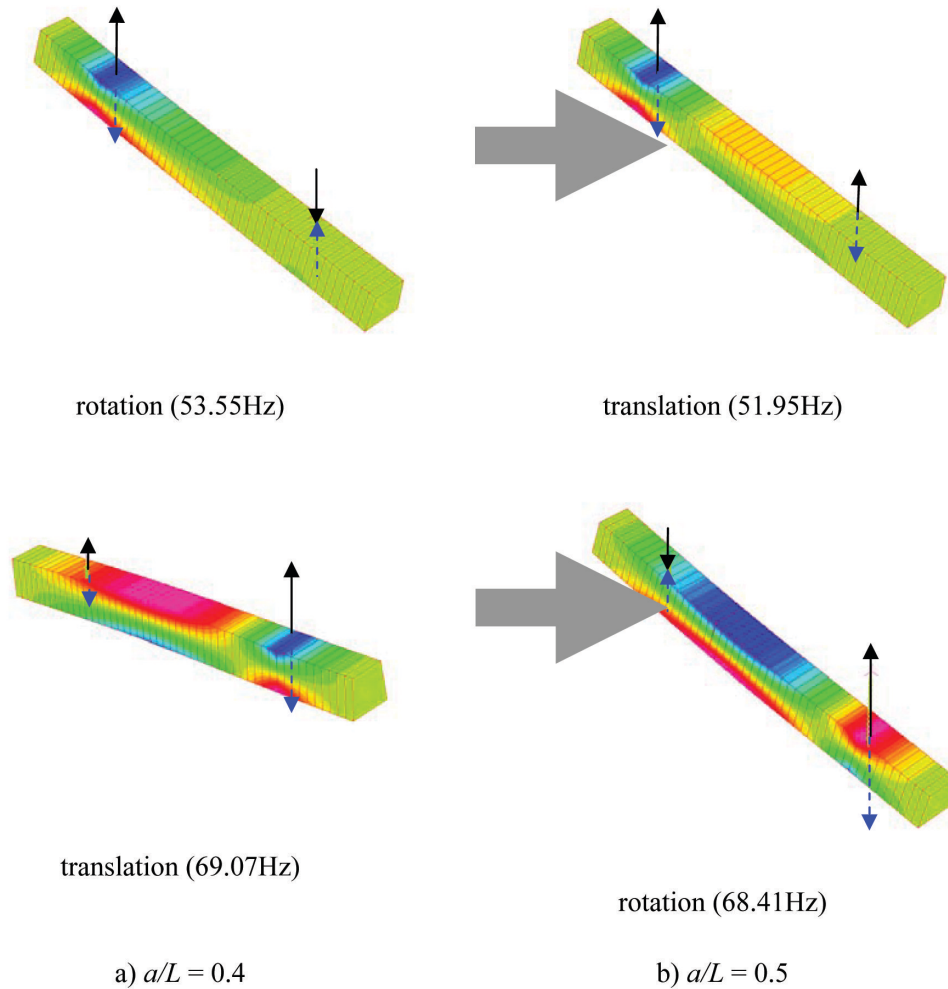


Figure 6. Transition of rigid body mode shapes

6. Conclusions

Free vibration characteristics of a type of voided railway concrete sleepers in a track structure system are investigated using both experimental modal testing and finite element approach. Modal testing was performed on an Australian-manufactured sleeper on a ballast test bed. The single-side hovering voids and pockets underneath sleeper were artificially created. Modal data are obtained from the experiments in order to investigate the capability of the simplified finite element analysis developed earlier for predicting free vibration behaviors of voided railway concrete sleepers. Either experimental or numerical results show that the voids and pockets have significant effect on the rigid body dynamics and the first bending vibration of the voided sleepers. However, the voids are unlikely to substantially affect the higher flexural modes of vibration. Nonlinear degree of dynamic softening and hardening due to voids and pockets can be detected not only in translation and rotation modes of vibration, but also found in the flexural modes of vibration. On the basis of both experimental and numerical

investigations, the finite element model has been proven to accurately predict the trend of dynamic behaviours of voided railway concrete sleepers. Thus, the health monitoring of railway sleepers with different void configurations can be investigated.

Importance of this study involves the development of dynamic health monitoring tool for in-situ concrete sleepers in the modern railway track using integrated vibration measurement and finite element model updating. It is found that using the vibration measurement provides high accuracy of the condition assessment of railway sleepers in track systems, since other methods for health monitoring of sleepers, e.g. radar, ultrasonic, microwave, or image analysis, could not properly detect voids underneath or cracks in sleepers. It should be noted that a voided or damaged sleeper may not much affect the global track responses but it may result in the dynamic overturning instability of tracks and the abnormal wheelset movements, of which further study is required. Nonetheless, this understanding into the effect of boundary condition will help indicate the influential parameters associated with impact loading and its effect particularly on track components.

Acknowledgement

The authors are grateful to acknowledge the Australian Cooperative Research Centre for Railway Engineering and Technologies for the financial support as part of Project #5/23. The test sleeper was kindly supplied by ROCLA. Many thanks go to the technical officers, particularly Alan Grant, for their assistance in the laboratory.

References

- Barke D.W., and Chiu W.K., (2005). "A review on the effect of out-of-round wheels on track and vehicle components," *Proceedings of the Institution of Mechanical Engineers Part F*, 219, 151-175.
- Cai Z., (1992). "Modelling of rail track dynamics and wheel/rail interaction," Ph.D. Thesis, Department of Civil Engineering, Queen's University, Ontario, Canada.
- Clark R.A., Dean P.A., Elkins J.A., and Newton S.G., (1982). "An investigation into the dynamic effects of railway vehicles running on corrugated rails," *Journal of Mechanical Engineering and Science* 24, 65-76.
- Dahlberg T., and Nielsen J., (1991). "Dynamic behaviour of free-free and in-situ concrete railway sleepers," *Proceedings of International Symposium on Precast Concrete Railway Sleepers*, Madrid, Spain.
- Esveld C., (2001). *Modern Railway Track*, second edition, The Netherlands, MRT-Productions.
- Friswell M.I., Mottershead J.E., (1995) *Finite Element Model Updating in Structural Dynamics*, The Netherlands. Kluwer Academic Publishers.
- Grassie S.L., and Cox S.J., (1984). "The dynamic response of railway track with flexible sleepers to high frequency vertical excitation," *Proceedings of Institute of Mechanical Engineering Part D* 198, 117-124.
- Grassie S.L., (1995). "Dynamic modelling of concrete railway sleepers," *Journal of Sound and Vibration* 187, 799-813.

- G+D Computing, (2002). Using STRAND7 Introduction to the Strand7 finite element analysis system, Sydney G+D Computing Pty Ltd.
- G+D Computing, 2005. STRAND7 Theoretical Manual, G+D Computing Pty Ltd.
- Kaewunruen S., and Remennikov A.M., (2005). "Applications of experimental modal testing for estimating dynamic properties of structural components," Proceedings of Australian Structural Engineering Conference 2005, Newcastle, Australia, [CD Rom].
- Kaewunruen S., and Remennikov A.M., (2006a). "Sensitivity analysis of free vibration characteristics of an in-situ railway concrete sleeper to variations of rail pad parameters," Journal of Sound and Vibration 298, 453-461.
- Kaewunruen S., and Remennikov A.M., (2006b). "Post-failure mechanism and residual load-carrying capacity of railway prestressed concrete sleeper under hogging moment," Proceedings of International Conference of Structural Integrity and Failure 2006, Sydney, Australia, pp. 331-336.
- Kaewunruen S., and Remennikov A.M., (2006c). "Rotational capacity of railway prestressed concrete sleeper under static hogging moment," Proceedings of 10th East Asia Pacific Conference of Structural Engineering and Construction, Bangkok, Thailand, Vol. 5, pp. 399-404.
- Kaewunruen S., and Remennikov A.M., (2007a). "Effect of improper ballast packing/tamping on dynamic behaviours of on-track railway concrete sleeper," International Journal of Structural Stability and Dynamics 7, 167-177.
- Kaewunruen S., and Remennikov A.M., (2007b). "Experimental and numerical studies of railway prestressed concrete sleepers under static and impact loads," Civil Computing Journal, AIT-ACECOMS, 25-28, invited.
- Kaewunruen S., and Remennikov A.M., (2007c). "Investigation of free vibrations of voided concrete sleepers in railway track system," Proceedings of the Institution of Mechanical Engineers Part F Journal of Rail and Rapid Transit, 221(4), 495-508.
- Kaewunruen S., and Remennikov A.M., (2008). "Influence of support conditions on flexural response of prestressed concrete sleepers," Journal of Concrete Institute of Australia, accepted.
- Knothe K., and Grassie S.L., (1993). "Modelling of railway track and vehicle/track interaction at high frequencies," Vehicle System Dynamics 22, 209-262.
- Kumaran G., Menon D., and Nair K.K., (2003). "Dynamic studies of railtrack sleepers in a track structure system," Journal of Sound and Vibration, 268, 485-501.
- Neilsen JCO., (1991). "Eigenfrequencies and eigenmodes of beam structures on an elastic foundation," Journal of Sound and Vibration, 145, 479-487.
- Plenge M., and Lammering R., (2003). "The dynamics of railway track and subgrade with respect to deteriorated sleeper support," In: K. Popp und W. Schiehlen (Ed.), System Dynamics and Long-term Behaviour of Railway Vehicles, Track and Subgrade, (Springer Verlag, pp. 295-314).
- Remennikov A.M., Kaewunruen S., (2005). "Investigation of vibration characteristics of prestressed concrete sleepers in free-free and in-situ conditions," Proceedings of Australian Structural Engineering Conference 2005, Newcastle, Australia, [CD Rom].
- Remennikov A.M., and Kaewunruen S., (2006). "Experimental investigation on dynamic sleeper/ballast interaction," Experimental Mechanics, 46, 57-66.
- Remennikov A.M., and Kaewunruen S., (2007). "A review on loading condition of railway track structures due to wheel and rail vertical interactions," Progress in Structural

- Engineering and Materials, incorporated in Structural Control and Health Monitoring, in press.
- Remennikov A.M., Murray M.H., and Kaewunruen S., (2007). "Conversion of AS1085.14 for prestressed concrete sleepers to limit states design format," Proceedings of AustRail Plus 2007 Conference, Australasian Railway Association, December 4-6, 2007, Sydney.
- Sadeghi J., (1997) "Investigation of characteristics and modelling of railway track system," PhD Thesis, School of Civil, Mining, and Environmental Engineering, University of Wollongong, Australia.
- Standards Australia, (2003). Australian Standard AS1085.14 Prestressed Concrete Sleeper, Standards Australia Ltd.

Note: The authors' publications can be reached electronically via the University of Wollongong Research Online at URL <http://ro.uow.edu.au>